Biomedicine & Pharmacotherapy 163 (2023) 114828

Contents lists available at ScienceDirect

Biomedicine & Pharmacotherapy

journal homepage: www.elsevier.com/locate/biopha

Maslinic acid solid lipid nanoparticles as hydrophobic anticancer drug carriers: Formulation, *in vitro* activity and *in vivo* biodistribution

Aixa Aguilera-Garrido [a,b,1,2], Pablo Gravánn [a,b,c,d,e,f,1], Saúl A. Navarro-Marchal [b,e,g], Marta Medina-O'Donnell [h], Andrés Parra [h], María José Gálvez-Ruiz [a,b], Juan Antonio Marchal [b,c,d,e,f,*], Francisco Galisteo-González [a,b,*]

[a] Department of Applied Physics, University of Granada, Fuentenueva, s/n, Granada 18071, Spain
[b] Excellence Research Unit Modelling Nature (MNat), University of Granada, Fuentenueva, s/n, Granada 18071, Spain
[c] Department of Human Anatomy and Embryology, Faculty of Medicine, University of Granada, Granada 18016, Spain
[d] Instituto de Investigación Biosanitaria de Granada (ibs.GRANADA), University of Granada, Granada 18012, Spain
[e] Biopathology and Regenerative Medicine Institute (IBIMER), Centre for Biomedical Research (CIBM), University of Granada, Granada 18016, Spain
[f] BioFab i3D, Biofabrication and 3D (bio)printing laboratory, University of Granada, Granada 18100, Spain
[g] Cancer Research UK Edinburgh Centre, Institute of Genetics and Cancer, University of Edinburgh, Edinburgh EH4 2XU, UK
[h] Department of Organic Chemistry, University of Granada, Fuentenueva, s/n, Granada 18071, Spain

ARTICLE INFO

Keywords:
Maslinic acid
Curcumin
Solid lipid nanoparticles
Poloxamer
Pancreatic cancer
Breast cancer

ABSTRACT

Maslinic acid (MA) is a natural pentacyclic triterpenoid with inherent antitumor activity which has a very low solubility in water. MA solid lipid nanoparticles (SLNs) were prepared using Poloxamer 407 and Dicarboxylic acid-Poloxamer 407 as surfactants. Both MA SLNs are monodisperse, with sizes around 130 nm, and stable. Curcumin has been encapsulated in both types of nanoparticles without altering their colloidal properties. Moreover, SLNs greatly improve the solubility of MA and Curcumin. The cytotoxicity of MA and SLNs has been evaluated in BxPC3 human pancreatic cancer cells, MCF7 human breast cancer cells, and in a human fibroblast primary cell line. MA shows higher cytotoxic effect in BxPC3 and MCF7 cancer cells than in human primary fibroblasts. Nile Red loaded MA SLNs are quickly uptaken by BxPC3 and MCF7 cells, and show different cytoplasmic distributions depending on the cellular line. The oral or intravenous administration of MA SLNs in mice does not report any toxic effect, and the intravenous administration of fluorescent MA SLNs shows a homogeneous distribution in mice, without site-specific accumulation. Results suggest the great potential of MA SLNs as nanocarriers of anticancer drugs and as promising targeted theranostic nanodevices.

1. Introduction

About half of all new drugs are natural compounds or directly derived from them, which evidence the outstanding role of natural products in drug discovery [1]. Maslinic Acid (MA), also known as crategolic acid or 2α, 3β-dihydroxyolean-12-en-28-oic acid, is a gaining interest molecule due to its multiple therapeutic potentials and lack of harmful effects [2,3]. MA is a phytochemical triterpene broadly distributed in nature [4], which can be extracted in large amounts from olive oil milling by-products following a simple and economic process. Different biological activities have been reported for MA such as hepatoprotective, analgesic, anti-inflammatory, antidiabetic, antimicrobial, and anti-human immunodeficiency virus (HIV) [5–8,9]. In addition, MA has antitumor potential, both in vitro and in vivo, rising great interest on the cancer research area [9–12–15–18]. However, its application presents a major drawback: its low solubility in aqueous solutions (3.6 $\mu g \cdot L^{-1}$) [9], which drastically reduces its bioavailability. This limitation explains the difficulties to transfer this promising compound from bench

* Correspondence to: Dpt. of Applied Physics, University of Granada, Fuentenueva s/n, Granada 18071, Spain.
E-mail addresses: jmarchal@ugr.es (J.A. Marchal), galisteo@ugr.es (F. Galisteo-González).
[1] These authors contributed equally to this work.
[2] Current address: Laboratoire Lorrain de Chimie Moléculaire (L2CM), UMR CNRS 7053, Équipe MolSyBio, Boulevard des Aiguillettes, 54506, Vandoeuvre-Lès-Nancy, France. Centre de Recherche en Automatique de Nancy (CRAN), UMR 7039, Institut de Cancérologie de Lorraine (ICL), 6 Av. de Bourgogne, 54519 Vandœuvre-lès-Nancy.

https://doi.org/10.1016/j.biopha.2023.114828
Received 24 February 2023; Received in revised form 14 April 2023; Accepted 30 April 2023
Available online 8 May 2023

to clinical applications. Different chemical approaches have been studied to improve MA solubility in aqueous medium, such as the generation of synthetic derivatives from MA [9–12,13,14]. Nonetheless, this impediment can also be addressed avoiding molecular alterations, by dispersing pure MA in the form of nanoparticles (NPs). Solid lipid nanoparticles (SLNs) were born in the nineties, as an alternative to nanoemulsion-based drug delivery systems to achieve a slower and more sustained drug release [19,20]. These colloidal systems are composed of lipids, which are solid at room and body temperature [21]. The solid lipids form a highly structured hydrophobic solid core, inside of which hydrophobic drugs can be incorporated [19,21,22]. The use of bioactive lipids such as MA in SLNs composition provides a functional nanocarrier that brings the possibility of establishing synergistic relations between MA and other(s) carried drug(s). Within this scenario, we present a comprehensive study on the synthesis and characterization of MA SLNs prepared by a solvent displacement method. This procedure, also known as nanoprecipitation technique, is a well-established, reproducible, and economic one-step manufacturing process that was firstly described and patented by Fessi *et al.* [23,24].

Poloxamer 407 (P407), also known by its commercial name PluronicTM F127, is a non-ionic surfactant categorized as a GRAS (Generally Recognized As Safe) excipient. In its structure we find three polymeric blocks, a central hydrophobic region composed of polypropylene oxide (PPO) flanked by two hydrophilic blocks of polyethylene oxide (PEO) [25]. P407 is widely used to build up NPs' and nanoemulsions' shells because it promotes colloidal stability by steric repulsion [26,27]. The main interest of P407 as a shell component rises from its ability to modulate the formation of the protein-corona, helping to reduce adsorption of blood proteins and mononuclear phagocyte system recognition, thereby, allowing NPs to remain in the systemic circulation for prolonged periods of time [28–30]. P407 can be modified to include carboxyl groups at both side ends of the polymeric chain (Dicarboxylic acid P407, PC407) [31]. This modification furnishes the SLNs surface with accessible carboxylic groups which can be used to further functionalize with other molecules via covalent linking [31].

With the help of these surfactants, P407 and PC407, we prepared colloidal dispersions of MA in the form of SLNs, and their colloidal characteristics and stability were analysed. To assess the possibility of using these MA SLNs as carriers of other drugs, curcumin (Cur) was encapsulated as hydrophobic drug model. This polyphenol is extracted from the rhizomes of *Curcuma longa*, it presents low bioavailability in its free form, and has probed anti-tumor, antioxidant, and anti-inflammatory activities [32]. We have tested the in vitro toxicity of these MA SLNs and Cur-MA SLNs in BxPC3 pancreatic cancer cells, MCF7 breast cancer cells, and in human primary fibroblasts, as well as the uptake of Nile Red (NR)-loaded MA SLNs by confocal microscopy and flow cytometry. The in vivo toxicity and biodistribution was evaluated to probe the safety and potential of the system.

2. Experimental section

2.1. Reagents

Cur ([CAS:458–37–7]), P407 (Pluronic F127, [CAS:9003–11–6]), NR and IR780 iodide were purchased from Sigma-Aldrich. PC407 was synthesized, and kindly donated, by Dr. A. Parra from the Organic Chemistry Dpt. of the University of Granada, as previously described [31]. 3-(4,5-Dimethylthiazol-2-yl)− 2,5-diphenol tetrazolium bromide (MTT) cell-proliferation kit was obtained from Promega (USA). Analytical grade ethanol, acetone and propanol were commercially supplied by Merck, and ethyl acetate by Scharlab. All aqueous solutions were prepared using ultrapure water from a Millipore Milli-Q Academic pure-water system.

MA was isolated from solid olive oil production wastes according to the method validated in the patent [3]. Briefly, MA was extracted successively in a Soxhlet with hexane and ethyl acetate. From this extraction, a solid residue consisting of a mixture of oleanolic acid and MA (20:80), was obtained. Both products were purified from the mixtures by column chromatography over silica gel, eluting with a dichloromethane / acetone gradient of increasing polarity, starting with 40/1 ratio. The separation was evaluated by thin layer chromatography and fractions are grouped by similar composition.

2.2. Cell lines and culture conditions

BxPC3 human pancreatic cancer, MCF7 human breast cancer cells lines were obtained from American Type Culture Collection (ATCC), and cultured following ATCC recommendations. Human primary fibroblasts were isolated by an enzymatic digestion using collagenase I (Sigma Aldrich) from skin tissue during abdominoplasty surgery (ethics committee reference: 0467-N-20) after obtaining written informed consent. MCF7 cells and fibroblasts were cultured in Dulbecco's Modified Eagle's Medium (DMEM). BxPC3 cell line was cultured in Roswell Park Memorial Institute 1640 Medium (RPMI) (Gibco, Grand Island, NY, USA). These cell lines culture mediums were supplemented with 10% (v/v) heat-inactivated fetal bovine serum (FBS) (Gibco), 1% L-glutamine, 2.7% sodium bicarbonate, 1% Hepes buffer, and 1% penicillin/streptomycin solution (GPS, Sigma). All cell lines were grown at 37°C in an atmosphere containing 5% CO_2 and 95% humidity. All cell lines were tested routinely for mycoplasma contamination.

2.3. Preparation of MA SLNs

MA SLNs were prepared by adapting a solvent-displacement method [23]. Briefly, an organic phase containing 3 mg · mL^{-1} of MA in a 1/1 mixture of ethanol and acetone was poured, under moderate stirring and at room temperature, into the same volume of an aqueous solution of P407 or PC407 at 1 mg · mL^{-1}, to produce PMA and PCMA respectively. The dispersion became turbid immediately after mixing both phases because of the formation of SLNs. Subsequently, the organic solvents were removed by rotary evaporation under reduced pressure at a temperature below 40°C. To clean the dispersion from excess surfactant, SLNs were thoroughly dialyzed against ultrapure water for 72 h changing water daily (300 kDa MWCO membranes). NR-loaded and IR780-loaded SLNs were also prepared for cellular uptake assays and for in vivo biodistribution assays, respectively. NR (0.1% w/w respect to MA) or IR780 (0.05% and 0.5%, w/w respect to MA), were dissolved in the organic phase along with the MA prior to the SLNs preparation. Fluorescent dye IR780, emitting in the infrared range of wavelength, was used for in vivo distribution assays to avoid interference with mice autofluorescence.

Cur-loaded SLNs were synthesized by dissolving Cur in the organic phase (0.2 mg · mL^{-1}) along with MA. Non-encapsulated Cur was separated by centrifugation at 1,000 g for 4 min at 20°C. The supernatant with the Cur-loaded SLNs was carefully collected. Cur concentrations were determined by diluting 20 μL of SLNs dispersions in 1 mL of propanol. Samples were then vortexed, incubated in an ultrasonic bath (15 min), and centrifuged at 21,000 g for 10 min at 20°C. The supernatants were collected and their absorbance measured at 430 nm using a UV-Vis spectrophotometer (BioSpectronic Kinetic Spectrophotometer Eppendorf, Germany). Cur concentration was calculated by appropriate calibration curve of free Cur in propanol ($R^2 > 0.99$). Each sample was measured in triplicate. Encapsulation Efficiency (*EE*) and Drug Loading (*DL*) were calculated as:

$$EE(\%) = \frac{\text{mass of entrapped Cur}}{\text{initial mass of Cur}} \times 100 \quad (1)$$

$$DL(\%) = \frac{\text{mass of entrapped Cur}}{\text{mass of MA}} \times 100 \quad (2)$$

2.4. Physicochemical characterization of MA SLNs

Hydrodynamic diameter (D_H), polydispersity index (*PDI*) and ζ-potential were determined by dynamic light scattering (DLS). Measurements were performed with a Zetasizer Nano-S system (Malvern Instruments, UK). The self-optimization routine in the Zetasizer software was used for all measurements, and the ζ-potential was calculated according to the Smoluchowsky theory. Samples were diluted 1/100 with a low ionic strength phosphate buffer (1.13 mM NaH_2PO_4, pH 7), stabilized for 30 min and measured at 25°C in triplicate. Results appear as the mean value ± standard deviation (SD).

The morphological characterization of SLNs was performed by Transmission Electron Microscopy (TEM) and Scanning Electron Microscopy (SEM). For TEM imaging, 25 μL of each sample were incubated on carbon-coated grids for 5 min before being washed off with ultrapure water. Uranyl acetate was employed for negative stained samples. Grids were observed in a LIBRA 120 PLUS from Carl Zeiss SMT operated at 120 kV with filament of Lanthanum hexaboride. SEM analysis was conducted by placing 80 μL of each sample on SEM stubs. FEG-ESEM QUEMSCAN 650 F at 30 kV was employed to observe the prepared samples. Sample preparation and visualization were done in the Scientific Instrumentation Centre of the University of Granada.

In order to study the pH, salinity and long-term colloidal stability, several experiments were performed. Ionic strength and pH effects were evaluated by titration experiments, using the Malvern MPT-2 Autotitrator together with the Malvern Zetasizer Nano-ZS. To analyse the ionic strength effect, SLNs were initially prepared in a 2 mM solution of KNO_3 at pH 7.2. Particles were then titrated, and D_H and ζ-potential measured concomitantly, from low ionic strength to 0.5 M using a 2 M solution of KNO_3. In the case of pH titrations, samples were brought to similar initial conditions of ionic strength (10 mM with KNO_3 1 M) and pH (11.0 with NaOH 1 M). Then, titration from pH 11 to pH 3 was carried out automatically by controlled additions of HNO_3 (25 or 50 mM). All experiments were initiated with a volume of 10 mL containing 0.6 mL of MA SLNs sample. The obtained data were analysed using Origin 8®software (OriginLab Corporation, Northampton, Massachusetts, USA).

The long-term stability of the SLNs was evaluated after storage at 4°C. As criteria for physical-stability, the particle D_H, *PDI*, and ζ-potential were determined by DLS, in a low ionic strength pH 7 buffer (1.13 mM NaH_2PO_4), at predetermined time points.

2.5. Quantification of MA and Cur from the SLNs for cellular assays

SLNs were diluted in a 1/100 ratio with distilled H_2O. 10 μL of diluted SLNs were added to 1 mL of 2-propanol, vortexed for 1 min and incubated on an ultrasound water bath for 10 min. Then, samples were centrifuged for 10 min at 21,000 g, the supernatant was collected and analysed by liquid chromatography electrospray ionization-tandem mass spectrometry (LC-ESI-MS/MS). Analytes were separated using ACQUITY UPLCr BEH C18 column (1.7 μm, 50 × 2.7 mm) equilibrated with 0.1% formic acid in H_2O and acetonitrile with 0.1% formic acid (50:50, v/v) at 40°C. Samples were kept at 20°C and 5 μL of sample were injected in the column. Analytes were eluted with a mobile phase consisting of acetonitrile with 0.1% formic acid at a flow rate 0.4 mL · min^{-1}. The MS analysis was performed in a Waters XEVO-TQS. Ion transitions were monitored with multiple reaction monitoring (MRM) in negative ionization mode for MA (m/z 471.58 > 393.34, and m/z 471.58 > 405.44) and in positive ionization mode for Cur (m/z 369.29 > 116.95, m/z 369.29 > 144.98, m/z 369.29 > 176.99, and m/z 369.29 > 285.22).

2.6. Proliferation assay

BxPC3 (4.5×10^3 cells/well), MCF7 (10^4 cell/well), and fibroblasts (4.5×10^3 cell/well) were seeded on 96 well/plates and allowed to grow overnight. Free MA and Cur samples were prepared on the appropriate culture medium (RPMI for BxPC3 and DMEM for MCF7 and fibroblast) with < 1% of dimethyl sulfoxide (DMSO). The sample combining MA+Cur had a ratio 15/1 (μM). All SLNs were diluted in the appropriate culture medium. The MA/Cur ratio for Cur-loaded SLNs used for the toxicity assays varied from 22/1–12/1 (μM). Cells with the corresponding incubation medium were used as negative (0%) inhibition controls, while wells with only incubation medium and no cells were used as positive (100%) inhibition controls. Cells were incubated for 72 h. Then, incubation medium was removed, cells were washed with PBS, and 100 μl of MTT (0.6 mM) were added per well. Plates were incubated again at 37°C, with an atmosphere of 5% CO_2, and 95% humidity, for 3 h. MTT was removed, cells were washed with PBS, and 100 μl of DMSO were added per well. Absorbance was recorded at 570 nm (HEALES MB-580 microplate reader, Bangladesh). Each sample was tested in triplicate and each experiment was replicated in three independent assays.

The Therapeutic Index (*TI*) of MA and Cur in BxPC3 and MCF7 was calculated for all tested samples as[33]:

$$TI = \frac{IC_{50}^{\text{fibroblasts}}}{IC_{50}^{\text{tumor cell line}}} \quad (3)$$

2.7. Cellular uptake of Nile Red-loaded SLNs

Cellular uptake of NR-loaded SLNs by BxPC3 and MCF7 cells was assessed by flow cytometry and confocal fluorescence microscopy. In order to perform the flow cytometry assay, cells (1.5×10^5) were seeded into Corning cell culture flasks (VWR, Spain). Once 80% cell confluence was obtained, cells were trypsinized and washed with PBS. Then, 1×10^6 cells were placed in tubes and incubated with PBS and NR-SLNs, at a MA concentration of 50 μM and in a final volume of 200 μL. Cells were incubated with the NR-SLNs for 5, 10, 15, 35, and 65 min. Then, cells were centrifuged at 1500 g for 5 min, washed with PBS twice, resuspended in 300 μL of PBS, and analysed by flow cytometry with FACS Canto II (FACS Canto II, Becton Dickinson, New Jersey, US) using the software FACS Diva 6.1.2 (Becton Dickinson) for data analysis.

Confocal microscopy images of living cells were taken with Zeiss LSM 710 inverted laser scanning confocal microscope and processed with Zen Lite 3.4 software. 1.7×10^4 BxPC3 cells and 3.5×10^4 MCF7 cells were seeded in 35 mm glass bottom IBIDI chambers (81158, INYCOM) and allowed to growth for 24 h. Cell nuclei were stained with Hoechst immediately before imaging cells. During the cellular uptake assay, IBIDI chambers were placed on a thermostatic chamber, which was kept at 37°C. NR-SLNs were added to the chamber at a final MA concentration of 50 μM, and live cells were imaged for 30 min. For imaging live cells at 24 and 48 h, cells were kept into the incubator. After 24 or 48 h, nuclei were stained with Hoechst and cells imaged as previously described. All experiments were performed in triplicate and replicated at least twice. Sterility evaluations of all nanosystems were performed prior to develop SLNs uptake studies in order to exclude possible biological contamination.

2.8. In vivo assay: subacute toxicity and biodistribution

All in vivo experiments were performed in male and female CD1 mice (Crl:CD1 (ICR)). Animal welfare and experimental procedures were carried out in accordance with the institutional Research Ethics Committee of the University of Granada and *'Junta de Andalucía'*, Spain (approval number 12/07/2019/127) and international standards (European Communities Council directives 86/609 and 2012/707/EU). All animals (n = 15) were maintained in a cage with a 12 h light-dark cycle, and they were manipulated in a laminar air-flow cabinet to keep to the specific pathogen-free conditions.

Subacute toxicity of SLNs was assayed in healthy CD1 mice (males and females) after oral and intravenous administration. Mice were daily

treated for 5 days. The oral dose of MA was 86.0 mg of MA · kg^{-1}, while 30.9 mg of MA · kg^{-1} were employed for intravenous administration. The oral administration of SLNs was performed in conscious animals by using the intragastric gavage (injected volume < 200 μL). The intravenous SLNs were administered in lateral tail veins (injected volume < 100 μL). As a control, two female and one male CD1 mice were administered with PBS. Weight, behavior, food consumption, and visual inspection of mice were evaluated for 12 days, being day 1 the day of the first administration of SLNs. After 12 days, animals were sacrificed by cervical dislocation and dissected to detect possible anomalies consequence of the MA SLNs administration.

Biodistribution assays were performed with CD1 male mice (n = 6). Mice were administered with fluorescent dye IR780-loaded SLNs (at concentrations of 0.05% and 0.5%, w/w ratio respect to MA). In both, oral and intravenous administration, 0.4 mg of MA were employed. Fluorescence was then recorded by IVIS® (Perkin Elmer) at different times (0, 6, 24 and 48 h). As a control, a mouse was intravenously or orally administered with PBS.

2.9. Statistical analysis

Data appears as the mean value ± standard deviation. Data pairs were analysed with Student's t-test (2 samples with equal variance, $p < 0.05$).

3. Results and discussion

3.1. Synthesis and characterization of MA SLNs

P407 and PC407 were used as surfactants to synthesize two types of MA SLNs, namely, PMA and PCMA, following a solvent-displacement method. We have evaluated the effect of different variables intervening in the production process in terms of the colloidal characteristics of the resulting SLNs (average D_H, PDI, and ζ-potential). Fig. 1(A-F) shows the effect of the volume ratio of aqueous phase/organic phase, the organic phase composition (ethanol/acetone ratio), and the MA/Poloxamer ratio in the colloidal characteristics of both types of MA SLNs, namely, PMA and PCMA.

To study the influence of the volume ratio between aqueous and organic phases, the volume of the aqueous phase was modified while maintaining all the other experimental conditions. Higher ratios between the two phases, aqueous and organic, resulted in smaller NPs, with a minimum at the ratio 3/1 (Fig. 1A). The technique used for the preparation of these SLNs is based on the Ouzo effect, where the balance between solvent, non-solvent, and solute, plays a crucial role on the nucleation and the consequent formation of SLNs. The volume ratio between aqueous and organic phases has been described to influence the size of particles prepared with this methodology [34]. When both phases are mixed, ethanol diffuses into the water and brings with it the dissolved MA, which still has some solubility on the mixed phase. When MA is no longer soluble, i.e., supersaturation occurs, nucleation and SLNs

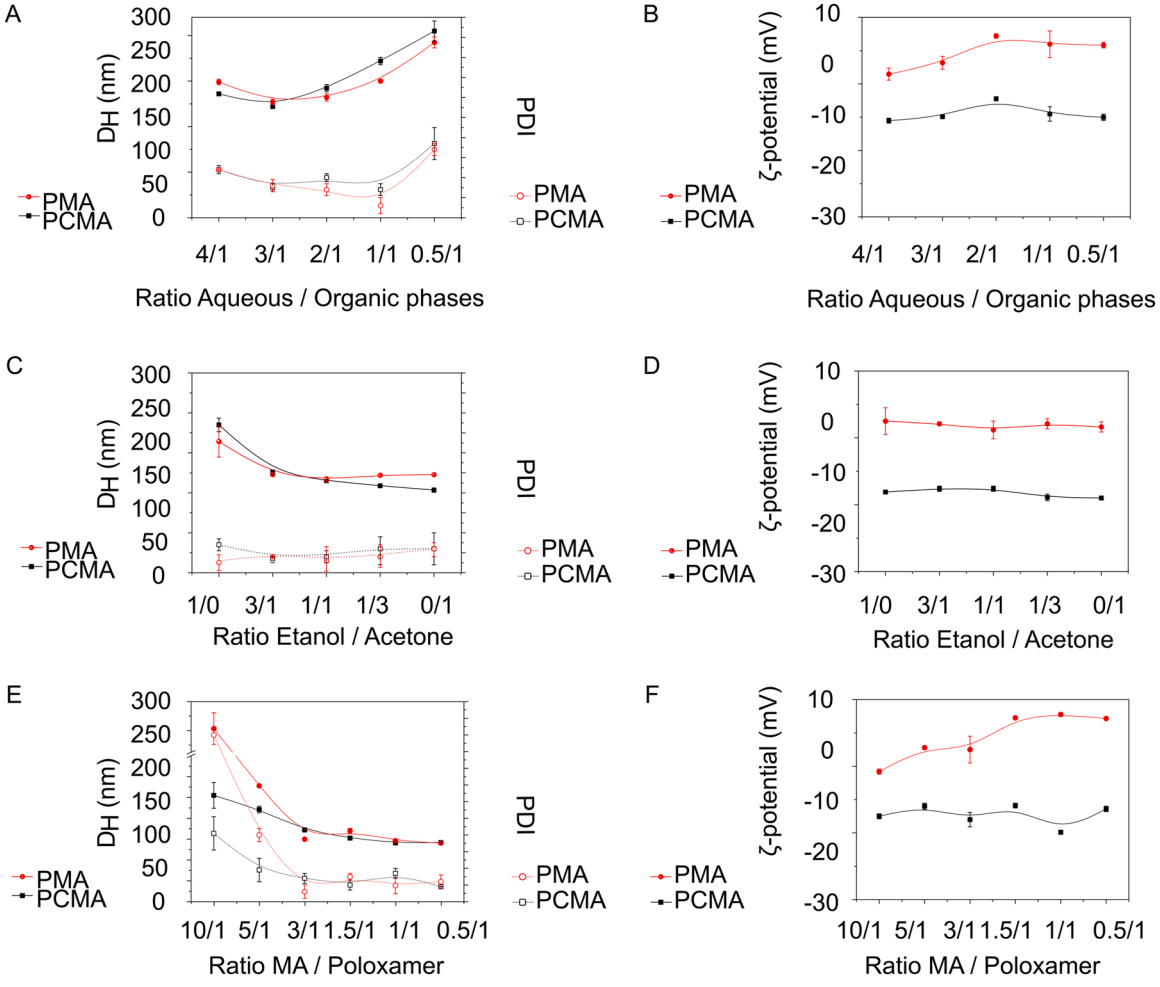

Figure 1. Physicochemical characterization of PMA and PCMA. To study the effect of different synthesis parameters on the D_H, *PDI*, and ζ-potential on PMA and PCMA, several experimental conditions were analysed: (A and B) ratio Aqueous phase/Organic phase, (C and D) ratio ethanol/acetone in the organic phase, and (E and F) ratio MA/Poloxamer. Data appear as the mean value of three measurements ± standard deviation.

formation starts. According to Classical Nucleation Theory, not all the formed nuclei are stable, and only those which have achieved the critical nucleus radius remain and can growth further [35]. Moreover, nucleation rate and critical nucleus radius depend on supersaturation, which is linked with the solubility of the hydrophobic solute on the mixed phase. An increase on the amount of water leads to a reduction of MA solubility on the mixed continuous phase, thereby to a sooner MA supersaturation and nucleation [34]. On the contrary, a higher solubility of MA would increase the critical nuclei radius, thus explaining the bigger D_H of SLNs observed when using a higher proportion of organic phase.

A decrease in D_H was also observed when acetone was included in the organic phase (Fig. 1C), suggesting that the size of the SLNs depends on the nature of the solvent used for their preparation. Solvents with lower viscosity have a higher diffusion coefficient, and have been suggested to promote a faster mixing of solvent and water, resulting in a more uniform supersaturation which leads to smaller particles [36–38]. According to this explanation, the lower absolute viscosity of acetone (3.16×10^{-4} Pa · s) compared to that of ethanol (10.95×10^{-4} Pa · s) may explain the decrease in size.

The effect of the ratio MA/Poloxamer was evaluated by changing the surfactant concentration on the aqueous phase. Fig. 1E shows that it is possible to obtain SLNs even at a very low poloxamer concentration (MA/ Poloxamer ratio of 10/1), when using PC407 as surfactant, although D_H and PDI values were high, 255 nm and 0.4, respectively. Employing the same ratio but P407 as surfactant, large aggregates were obtained. An increase in the proportion of poloxamers led to a decrease in D_H and PDI values. The rise in surfactant concentration affects nucleation by limiting the growth of NPs and stabilizing the system faster. On the same line, Lannibois *et al.* reported that the increase of stabilizer concentration for a given amount of hydrophobic compound led to smaller-sized SLNs [39]. As we have previously mentioned, the nucleation rate and critical nuclei radius are influenced by the supersaturation point. In this context, the interfacial tension of the particles/solution interface should be crucial on determining those parameters [35]. Therefore, the changes observed on D_H could also be ascribed to variations on the interfacial properties of the growing MA SLNs. Effectively, we have observed that a higher poloxamer concentration, with its concomitant interfacial tension reduction[27], leads to smaller-sized SLNs (Fig. 1E). ζ-potential of the PCMA prepared with different MA/Poloxamer ratios remains approximately stable (Fig. 1F). Nevertheless, ζ-potential from PMA reduced its negative value almost to 0 mV as the poloxamer concentration increases. It is noteworthy to mention that PMA presents a slight negative charge, considering that P407 is a non-ionic surfactant with no effective charge. This negative charge arises from the carboxyl groups of the MA molecules in the SLNs core. A reduction in the MA/Poloxamer ratio is translated into a higher amount of neutral poloxamer available to fill the SLNs surface; hence, we observe a reduction on ζ-potential possibly due to a higher concentration of P407 on the shell, which may screen more efficiently the MA carboxyl groups. Saturation seems to be achieved at a ratio around 1.5/1. The excess of poloxamer above this concentration remains in the aqueous solution and does not contribute to stabilize the SLNs [39]. Reducing the MA / Poloxamer ratio below this point does not further affect D_H, PDI or ζ-potential values.

Keeping in mind possible biomedical applications and subsequent scale up and industrialization, the effects of pH, ionic strength (NaCl, from 0 to 100 mM) and temperature (10, 25, and 50°C) of the aqueous phase were also evaluated. Results are summarized in Figure SM1 and show that these parameters had not significant effects in the colloidal characteristics of MA SLNs.

We finally defined a standard protocol to prepare the NPs used in subsequent experiments, which provided PMA with a D_H of (133 ± 3) nm, a PDI of (0.10 ± 0.02) and a ζ-potential of (− 6.5 ± 0.6) mV at pH 7; and PCMA with a D_H of (133 ± 3) nm, a PDI of (0.13 ± 0.04) and a negative ζ-potential of (− 20.2 ± 1.1) mV at pH 7. These conditions were 1/1 aqueous phase/organic phase volume ratio, 1/1 ethanol/acetone ratio, and 3/1 MA/Poloxamer ratio. SEM and TEM micrographs (Fig. 2A and B) of these preparations showed that particles are spherical or near spherical in shape, and homogeneous in size distribution, confirming DLS data.

The colloidal stability of the SLNs was evaluated at different ionic strength (Fig. 3A and B) and pH values (Fig. 3C and D). The effect of the ionic strength of the medium on D_H and ζ-potential was analysed varying the concentrations of KNO_3 at a stable pH of 7.2. As expected, as the ionic strength of the medium increases, electrolytes cause charge screening in the surface of the SLNs, which is translated to a decrease in ζ-potential absolute values (Fig. 3B). SLNs experienced a drastic reduction in their ζ-potential at low ionic strength, reaching stable values around 50 mM in the case of PMA, and 100 mM KNO_3 for PCMA. The different ζ-potential plateau values reached by both SLNs (around − 2 mV and − 5 mV for PMA and PCMA, respectively) seems to be related to the carboxyl groups present in PC407, some of which may be hindered and, consequently, it is difficult for counterions to neutralize them. However, despite the ζ-potential reduction, the D_H of both MA SLNs remained practically unaltered, evidencing the steric stabilization afforded by poloxamers (Fig. 3A).

The effect of pH on the ζ-potential of the SLNs was studied by performing a pH titration in a low ionic strength media (10 mM KNO_3). As shown in Fig. 3D, at basic pH values carboxyl acid groups are totally deprotonated, causing a negatively charged surface as reflected in the negative values of ζ-potential. When pH decreases over 8–7, acidic groups start to be titrated and protonated, thus reducing ζ-potential constantly till values close to 0 at acid pH. The more negative ζ-potential of PCMA compared to PMA is due to the presence of carboxylic groups in PC407.

With the aim of studying the stability in time of the MA SLNs, they were stored at 4°C and their colloidal parameters measured every 30 days for 5 months (Table SM1 from the supplementary information). As we can see in there, D_H, PDI and ζ-potential remained stable, probing the long-term stability of these colloidal systems.

The possibility of using these MA SLNs as nanocarriers of other drugs was evaluated by encapsulating Cur in both types of SLNs. Cur was incorporated during the synthesis process as part of the organic phase as described in the Section 2.3. Several MA/Cur ratios were assayed, being 3/0.2 the one with more satisfactory drug loading (*DL*) and encapsulation efficiency (EE). These values, as well as the colloidal parameters of the Cur-loaded SLNs, namely Cur-PMA and Cur-PCMA, are presented in Table SM2 from the supplementary information. As it can be observed, the incorporation of Cur had no significant effect on the size and dispersity of the SLNs. Cur-loaded SLNs were stored at 4°C and their Cur content, expressed as a percentage of the initial content, was determined at different time points (Fig. 2C). A significant Cur release was noticed after the first 24 h: about 12% in the case of Cur-PMA, and 8% in Cur-PCMA. Later on, and up to 60 days, Cur content remained practically constant and, in both systems, above 80% of the initial amount. Burst release effects, i.e., an extensive drug release from the nanocarrier after the synthesis process or after placing the system in the release medium, are usual in drug delivery systems [40]. Müller *et al.* claim that drug release is related to the structure of the lipid core, where solid lipids form crystals and the drug is excluded from the highly structured media [41]. During crystalline core formation, drug is rejected from the nanocarrier or is located close to the surface.

3.2. Proliferation assay and in vitro cytotoxicity

The in vitro toxicity of PMA and PCMA, as well as their Cur-loaded derivatives, Cur-PMA and Cur-PCMA, and the free compounds MA, Cur, and MA+Cur (dissolved in DMSO), was assayed in two human cancer cell lines, namely pancreatic BxPC3 and estrogen-receptor-positive breast MCF7, and in a healthy human fibroblast primary cell line. Results are summarized in Table 1 in the form of half maximal

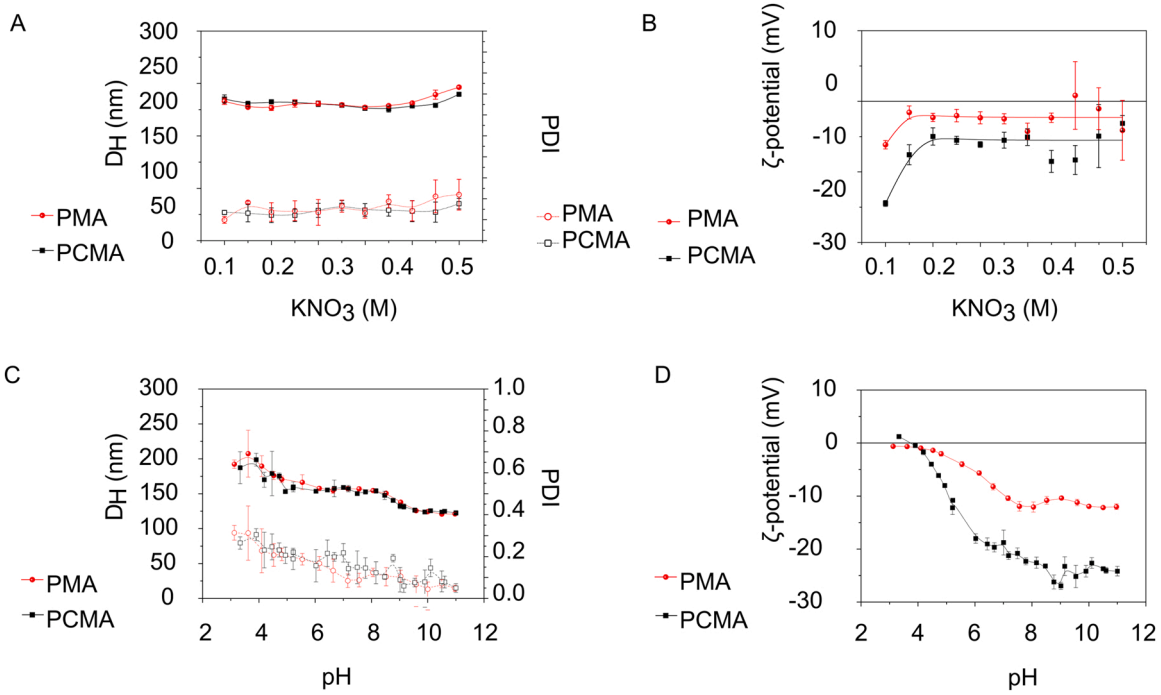

Figure 2. (A) Scanning Electron microscopy and (B) Transmission Electron microscopy of PCMA. (C) Cur retention with time at 4°C.

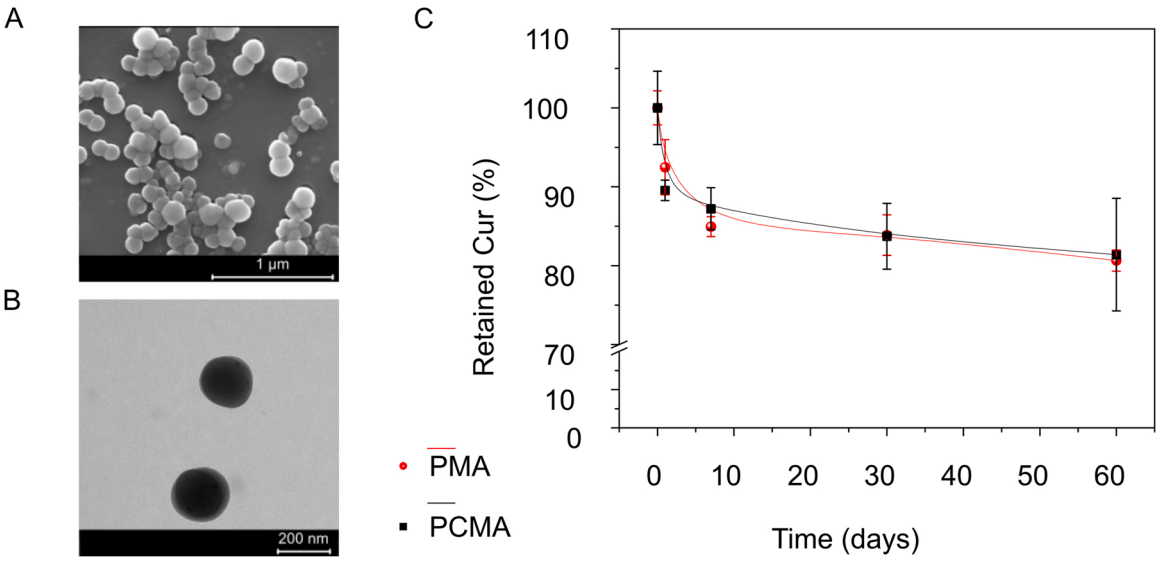

Figure 3. Colloidal stability of PMA and PCMA at different environmental conditions: (A and B) ionic strength (increasing concentrations of KNO_3, at a stable pH of 7.2), and (C and D) pH (10 mM KNO_3). Data appear as the mean value of three measurements ± standard deviation.

inhibitory concentration (IC_{50}) values and therapeutic index (TI, ratio between IC_{50} in the non-tumor cell line respect to a tumor cell line). The Figure SM2 from the supplementary information shows a graphic representation of the IC_{50} values reported in this table, and Figures SM3, SM4, and SM5 include the doses/effect sigmoidal fittings used to find these IC_{50} values. As we can see in Table 1, MA and Cur as free compounds had more harmful effect in BxPC3 than in fibroblasts, as the TI values for these compounds reflect, 2.0 and 2.4 respectively. In MCF7, the cytotoxic effect of MA was also higher than in fibroblasts, with a TI value in of 1.5, while Cur exerted similar effects in both cellular types. These results suggest that MA had a more selective cytotoxic effect against BxPC3 and MCF7 cancer cells than against healthy human primary fibroblasts. On the other hand, we can observe that the IC_{50} of Cur is approximately 5 times lower than the IC_{50} of MA in the tested cells lines. The cytotoxic effect of MA+Cur as free compounds was assayed in the molar ratio of 15/1 to maintain the Cur-loaded SLNs proportion. This combination reported the same IC_{50}^{MA} than the free MA alone in the three cell lines. From these results we concluded that the cytotoxic effect of MA was predominant owing to the higher proportion of MA compared to Cur, and therefore the effect of Cur was not measurable. At this drug ratio, we did not observe a synergistic effect between these two compounds.

The values of IC_{50}^{MA} reported for MA SLNs in BxPC3, MCF7, and fibroblasts were similar to the IC_{50} reported for free MA in the respective cell line. Therefore, MA SLNs formulation did not entail a modification of the cytotoxic effect of the compound. Similarly to the MA+Cur

Table 1
Half maximal inhibitory concentration (IC_{50}, μM) and therapeutic Index (TI = IC_{50} non-tumor cell line/IC_{50} tumor cell line) of MA, Cur and MA+Cur (as free drugs in DMSO or encapsulated) in BxPC3, MCF7 and fibroblasts.

	BxPC3			MCF7			Fibroblasts	
Treatment	IC_{50}^{MA}	IC_{50}^{Cur}	TI	IC_{50}^{MA}	IC_{50}^{Cur}	TI	IC_{50}^{MA}	IC_{50}^{Cur}
AM	42 ± 7		2.0	57 ± 8		1.5	83 ± 11	
Cur		6 ± 1	2.4		13 ± 3	1.1		15 ± 2
AM-Cur	45 ± 7		1.8	69 ± 1		1.2	81 ± 9	
PCMA	29 ± 7		1.5	47 ± 5		1	46 ± 12	
PCMA-Cur	40 ± 15		1.7	54 ± 6		1.3	68 ± 4	
PMA	34 ± 5		2.4	54 ± 11		1.2	58 ± 20	
PMA-Cur	52 ± 1		1.0	53 ± 14		1.0	54 ± 17	

combination as free compounds in DMSO, the Cur-loaded SLNs reported the same IC_{50}^{MA} than free MA. As in that case, the inclusion of Cur in the MA SLNs did not seem to improve the cytotoxic effect of MA. Nonetheless, the Cur loading capacity obtained for Cur-PMA and Cur-PCMA (around 6%) proved the potential of this systems as nanocarriers for hydrophobic drugs. This also supposed an improvement of Cur solubility, which is a limiting factor for the oral bioavailability of Cur, together with its extensive metabolization in the intestine and liver [42]. The encapsulation of Cur is a widely studied solution for both problems, since NPs allow the solubilization and administration of higher doses of bioaccesible Cur, i.e., absorbable at intestinal level, as well as they prevent its degradation. These factors contribute to increase the bioavailability of Cur [43]. Similarly, the main factor limiting the bioavailability of MA is its low solubility in water ($3.6\ \mu g \cdot L^{-1}$) [44]. The formulation in the form of SLNs allows the solubilization of MA up to $7\ mg \cdot mL^{-1}$, an increase of more than a million. It is the first time, that we know of, that MA has been used to produce NPs. Therefore, the improvement of the solubility of MA and Cur provided by these SLNs can be translated into a higher bioavailability of both compounds, allowing its administration and use as anticancer therapy. The use of NPs as drug delivery systems also offers the advantage of tumor targeting. This can be achieved by a passive mechanism, thanks to the enhanced permeation and retention (EPR) effect in the tumor, or by an active mechanism thanks to the functionalization of the NP with ligands which specifically recognize tumor cells. The EPR effect and the clearance mechanisms allow the preferent accumulation of NPs within a range 20–200 nm in the tumor area [45,46]. SLNs prepared in this work have 120–150 nm at pH 7 and are stable under a wide range of pH and ionic strength conditions (Fig. 3A and C). Moreover, PCMA have free carboxyl groups at the interface that provide available chemical reactive groups for the covalent coupling of targeting ligands, which would allow the development of targeted drug delivery systems.

Finally, the potential benefitial effect of MA for the treatment of cancer has been reported at different levels. MA has antioxidant and anti-inflammatory activities [4]. In vitro, MA has been reported that to recruit macrophages to the tumor microenvironment and promote their differentiation toward the M1 phenotype, which is related to a better prognosis in cancer [47]. And in vivo, the intraperitoneal injection of MA ($32\ mg \cdot kg^{-1}$ in DMSO) in BALB/c leukemic mice reported immunomodulatory activity and improved animals' survival. MA induced macrophage phagocytosis and increased natural killer activity [15].

Moreover, the intake of MA has been correlated to a muscle mass gain and prevention of muscle mass lost in elderly state and muscle atrophy models. Therefore, MA could promote a better patient condition in cancer patients [48–51] On the other hand, in vivo, the oral administration of MA has proved a chemopreventive role by preventing the appearance of preneoplastic induced lesions in the colon of rats [52], while in vitro MA has shown cytotoxic effects in several tumor cell lines, including A549 lung cancer cells [53], HT29, Caco-2, HCT116 and SW480 colorectal cancer cells [54–57], T24, TCCSUP, 253 J, and RT4 bladder cancer cells [58], ACHN, Caki-1, and SN12K1 renal cell carcinoma [59], and Panc1 and Patu-8988 pancreatic cancer cells [60]. MA has also been reported to sensitise tumor cells to certain drugs. For instance, MA potentiates the effect of gemcitabine in human gallbladder cancer cells [61], the effect of TNF-α in Panc-28 pancreatic cancer [62], and the effect of docetaxel in MDA-MB-231 [63]. Therefore, PMA and PCMA provide a nanocarrier with inherent biological activity which can have beneficial effects against the tumor and in the tumor microenvironment.

3.3. Cellular uptake of MA SLNs

The cellular uptake of these SLNs by pancreatic BxPC3 and breast MCF7 cancer cells was evaluated with NR-loaded MA SLNs (namely, NR-PMA and NR-PCMA) by flow cytometry (Fig. 4) and confocal microscopy (Fig. 5). Flow cytometry results showed that both NR-PMA and NR-PCMA, clearly enter in the two types of cells, BxPC3 (Fig. 4A) and MCF7 (Fig. 4B), after short incubation time periods (5 min). Both NR-SLNs continued entering in the cells up to 60 min after the incubation. Only in the case of NR-PCMA in MCF7 cells, saturation occurs after 30 min, with no significant variation at 60 min. We found significant differences when comparing fluorescence intensity between both types of cells and also between both types of SLNs. The uptake was higher in BxPC3 than in MCF7 (same SLN and incubation time). In agreement with our results, examples of NPs that show different uptake levels depending on the cellular line have been described. For instance, in a study, MCF7 cells were found to internalize 98 nm aggregated gold NPs better than 15–45 nm monodisperse gold NPs, while the uptake of gold NPs and aggregated gold NPs was the same in HeLa and A549 cells. Moreover, the uptake mechanism for 98 nm gold NPs was dependent of transferrin receptor-mediated endocytosis in HeLa and A549 cells, but it was not dependent of this endocytosis mechanism in MCF7 [64]. On the other hand, the fluorescence intensity of NR-PCMA was higher than that of NR-PMA in most of the times assayed and for both cell lines. Despite the more negative ζ-potential of NR-PCMA (-29 ± 3 mV) compared to NR-PMA (-16 ± 5 mV) at pH 7, the former seems to enter faster in both types of cells, MCF7 and BxPC3. It is widely accepted in literature that positively charged NPs are up taken by cells better that negatively charged or neutral NPs, owing to the electrostatic interactions stablished between the positively charged NP and the negatively charged cell membrane [65]. However, there are also many examples where NPs with a strong negative charge are also effectively up taken by cells, showing the complexity of the cell-NP interaction and the need of taking into consideration other parameters such as size and shape of the NP, hydrophilicity/hydrophobicity balance, NP coating or protein-corona. In this sense, Sánchez-Moreno *et al.* compared lipid oily-cored NPs with different shells: P407, Epikuron 145 V (E145, phospholipids), and two E145 + P407 mixes. The cellular uptake of these NPs by A549 cancer lung cells depended on the shell composition and it was reduced as the concentration of P407 in the shell was increased. They ascribed these differences to the higher hydrophobicity of the shell and to the less developed protein-corona in P407 NPs [66]. Similarly, the P407 coating of PMA could contribute to the formation of a less developed protein-corona, and therefore to a slower uptake, while the higher charge of PCMA could facilitate the establishment of electrostatic interactions with the surrounding proteins and to the formation of a more developed protein-corona, and in consequence, to a higher uptake of PCMA.

Confocal fluorescence images (Fig. 5) showed the fast uptake of both MA SLNs, NR-PMA and NR-PCMA, by BxPC3 and MFC7 cells, in agreement with the previously presented flow cytometry results. One minute after adding the NR-SLNs to living cells we observed red

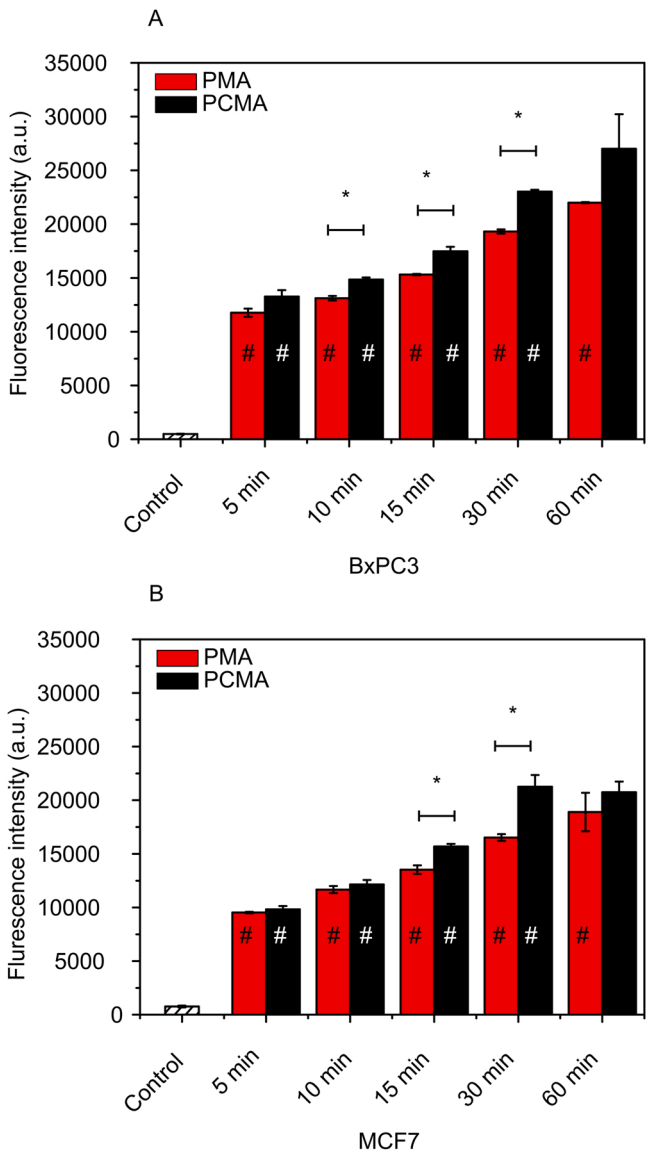

Figure 4. Cellular uptake of NR-PMA (red) and NR-PCMA (black) by (A) BxPC3 pancreatic cancer cells and (B) MCF7 breast cancer cells. Cells without SLNs were used as fluorescence intensity controls. Statistically significant differences between cells incubated with NR-PMA and NR-PCMA for the same time point are highlighted with '* ' and significant differences between BxPC3 and MCF7 for the same time point are highlighted with '#' (Student's T-test, 2 tails, 2 samples equal variance, $p < 0.05$).

fluorescence in the cytoplasm of both types of cells. The fluorescence intensity increased continuously with the incubation time, and it was clearly higher in BxPC3 pancreatic cancer cell line compared to MCF7 breast cancer cell line from 5 min onwards. At short incubation times (1 up to 20 min), the NR was distributed within the whole cytoplasm, surrounding the cell nuclei, and some differences were appreciated between BxPC3 and MCF7 cells regarding cytoplasmic accumulation of fluorescence. After 5 min of incubation, the red fluorescence was more homogeneously distributed in the MCF7 cell cytoplasm than in BxPC3, which presented brighter red cytoplasmic spots. At this incubation time, we observed cytoplasmic vesicles with high fluorescence intensity which were especially abundant in BxPC3 cytoplasm. After 20 min of incubation, red fluorescence was more evenly distributed within the whole cytoplasm of both cellular lines.

After longer incubation times, 24 and 48 h, fluorescence intensity sharply decreased, very probably because of the degradation inside the cell cytoplasm and/or the exclusion out of the cells. In these images, the NR fluorescence can be appreciated as restricted to some cytoplasmic areas, especially in BxPC3, where it was accumulated near the cytoplasmic membrane. At these long incubation times we found that some red fluorescence spots corresponded to cytoplasmic vesicles. The co-localization of vesicles and NR fluorescence was more evident in MCF7 cells. The peripheral localization of fluorescence in BxPC3 could indicate that the cells were excluding NR. In fact, one of the resistance mechanisms described in cancer cells consist in including anticancer drugs in microvesicles for its exocytosis [67].

There exist different mechanisms for NPs to enter the cells. Endocytic mechanisms are commonly the preferred entry way, but passive diffusion or entry through hole formation are also possible [68]. Poloxamer 188 coated SLNs (30 nm, 60 nm and 150 nm) have been shown to enter the cells from bovine olfactory and nasal respiratory tissues through different endocytic pathways, but also through non-endocytic and non-energy dependent mechanisms, although in a lesser extent [69].

On the other hand, Chai and coworkers found that the transport of Glycerol monostearate SLNs across Caco-2 differentiated and polarized monolayers was mediated by macropinocytosis pathway and clathrin- and caveolae-related routes [70]. Therefore, different mechanisms have been proposed for the entrance of SLNs into cancer cells. The different uptake performance of PMA and PCMA, as well as the fluorescence localization depending on the two cell lines, could mean a different interaction SLNs-cell, including different uptake mechanism and trafficking inside the cell.

3.4. *In vivo subacute toxicity of PCMA*

With the aim of assessing the in vivo effect of MA administered in the form of SLNs, male and female CD1 (Crl:CD1(ICR) mice were treated with PCMA at doses increasing from 52 up to 86 mg of MA · kg^{-1} for oral administration, and from 19 up to 31 mg of MA · kg^{-1} for intravenous administration.

A 5-days administration period was chosen to test the subacute toxicity of SLNs [71]. We assayed only PCMA because they were the best performing SLNs, with functionalization possibilities, and in order to minimize the number of treated mice. Fig. 6 shows the weight of the mice treated with the highest concentration of MA SLNs during the 5 days of treatment and the 7 following days (Fig. 6A and B). Results showed that mice's weight did not suffer abnormal variations and they did not show any strange change in the behavior, food or water consumption, or signs of toxicity such as loss of movement, piloerection, or facial signs of pain during the 12 days that animal remained under surveillance. After this period, mice were sacrificed by cervical dislocation and necropsies did not show any macroscopic anomaly (Figure SM6 from supplementary information). MA is a non-toxic compound which has probed its multiple beneficial effects in health, such as neuro and cardioprotective, anti-inflammatory, antioxidant, antiparasitic activities and its protective role in cancer [4]. Moreover, previous studies demonstrated that the oral administration of MA did not report any harmful effect in Swiss CD-1 male mice nor in Sprague-Dawley rats [2,72]. Our results indicated that PCMA had not toxic effect in healthy mice when orally or intravenously were administered.

3.5. *In vivo biodistribution of IR780-PCMA*

The biodistribution of the SLNs, in particular PCMA, after in vivo oral and intravenous administration to mice, were performed by using SLNs prepared with the fluorescent dye IR780. It was included at two different concentrations (0.05% and 0.5% w/w with respect to MA). CDR1 male mice were treated with IR780-PCMA and analysed with an IVIS fluorescence technique at times 0 h, 6 h, 24 h and 48 h after administration. IR780-PCMA did not report any harmful effect (Fig. 7). Intravenous IR780-PCMA-0.05% did not provide any fluorescence signal; however,

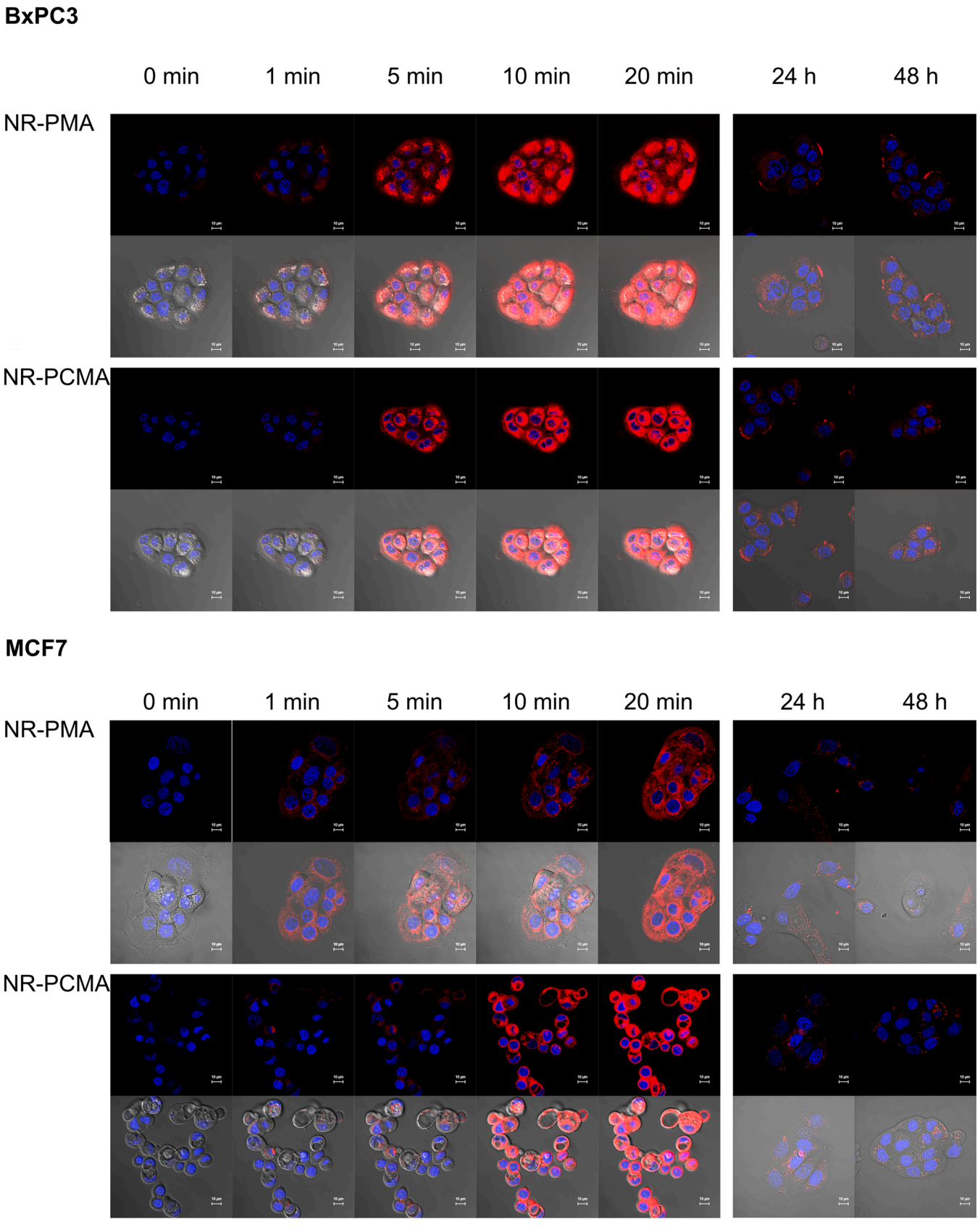

Figure 5. Confocal fluorescence microscopy images of living BxPC3 pancreatic cancer cells and MCF7 breast cancer cells incubated with NR-PMA and NR-PCMA at different times. Nuclei were stained with Hoechst immediately before the experiment and appear in blue. NR-PMA or NR-PCMA were added at a MA final concentration of 50 μM. NR fluorescence appears in red. Scale bars 10 μm.

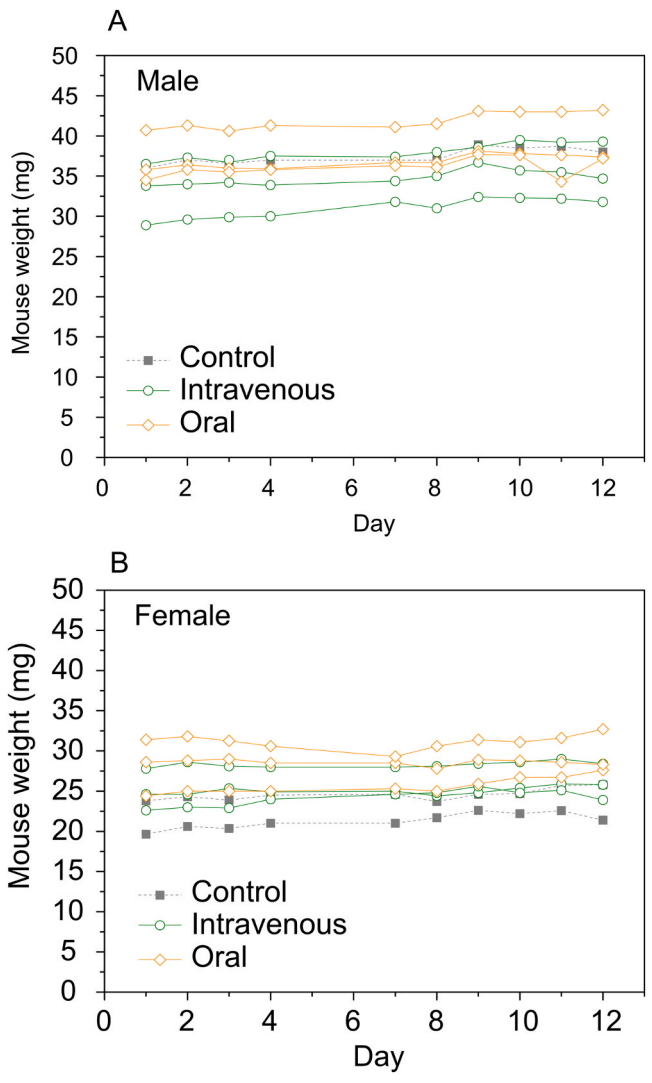

Figure 6. Toxicity of PCMA in healthy CD1 (Crl:CD1(ICR)) mice (male and females) after oral or intravenous administration. Weight of (A) males and (B) female mice was recorded for 12 days, starting the day of the first PCMA dose administration. Oral administration (orange line and diamonds), intravenous administration (green line and circles), and PBS control (grey line and squares).

SLNs with ten times more dye (0.5%), reported signal immediately after administration (0 h). At longer times, and up to 48 h, the fluorescence signal remained strong and spread through the whole mouse body. We did not observe in these images intensity accumulation in liver or spleen, which suggests that IR780-PCMA are not especially cleared from circulation by the reticuloendothelial system. Polyethylene glycol (PEG) and PEG containing polymers, such as poloxamers, have been probed to reduce the adsorption of proteins, including opsonins, to the NPs surface, which help them to escape from the reticuloendothelial system. This way, these polymers promote longer blood circulations times [73].

In the case of oral delivery, both IR780-loaded SLNs provided fluorescence signal immediately after their administration in the abdominal region, fitting the stomach and the beginning of the small intestine area (Fig. 7). The fluorescence intensity was higher for IR780-PCMA-0.5%, as expected from the higher IR780 concentration. 6 h after administration, there was a fluorescence intensity decay for both IR780-PCMA. However, the detected signal for IR780-PCMA-0.5% spread to the abdominal area matching the gastrointestinal region. After 24 h not signal for IR780-PCMA-0.05% was found and the signal intensity decayed for IR780-PCMA-0.5%. None of the samples reported any signal 48 h after the IR780-PCMA administration. The lack of signal outer the gastrointestinal region in Fig. 7 indicated that most of IR780-PCMA were eliminated through the feces. However, the lack of fluorescence signal in the whole animal (like in the IR780-PCMA-0.5%) does not mean that a part of IR780-PCMA have not arrived to the blood stream. In a previous study, MA orally administered in an aqueous solution of (2-hydroxypropyl)- β-cyclodextrin (40%, w/v) and sodium carboxymethylcellulose (0.5%) reported a bioavailability of 5.13% 30 min after intake in Swiss CD-1 mice [2]. And in vitro, MA in the form of SLNs has also been reported to cross Caco-2 and Caco-2/HT29-MTX intestinal epithelium models, although the permeability of the compound was low (about 2%) [74]. The low oral bioavailability can be the responsible of the lack of fluorescence signal. The IR780 concentration in blood might have not been enough to be detected, as in the case of intravenously administered IR780-PCMA-0.05%. However, our results show that, despite the cytotoxic effect reported in tumor cells, PCMA are save for oral and intravenous administration. In addition, the broad biodistribution of intravenous PCMA suggests that they are not cleared from blood circulation by the reticuloendothelial system. Therefore, SLNs represent a potential nanocarrier for the administration of drugs against cancer allowing the drug accumulation in the target tumor and reducing the side effect derived from nonspecific chemotherapy drugs.

4. Conclusions

We have defined a protocol to successfully prepare MA in the form of SLNs dispersed in water, stabilized with P407 or PC407. The procedure is a solvent-displacement method that produces highly stable and monodisperse MA SLNs. Both SLNs were stable in a wide range of pH and ionic strength conditions, as well as over time (up to 5 months). The main parameters defining the size of the SLNs were MA/poloxamer ratio, aqueous phase/organic phase ratio, and organic phase composition (ethanol/acetone ratio). Cur, as hydrophobic drug model, was effectively encapsulated in both MA SLNs, revealing the potential of this system as drug nanocarrier. After an initial burst release (day 1 after preparation), the Cur loading did not suffer great changes.

Free MA and MA SLNs showed a favorable TI (TI $>$ 1) for BxPC3 pancreatic cancer and MCF7 breast cancer cells, indicating that MA can be beneficial in treating both types of cancer, especially in pancreatic cancer, since higher TI values were found for BxPC3. It could be further improved using MA SLNs for encapsulating lipophilic drugs commonly used in clinic for treating this type of cancer. NR loaded MA SLNs were up taken by BxPC3 and MCF7 cells at short incubation times (1–5 min). Flow cytometry and confocal microscopy showed that NR-SLNs entered quickly into cells, and they did it faster and to a greater extent in the pancreatic BxPC3 cell line. After 24 h and 48 h, fluorescence intensity of NR-SLNs decreased in both cell lines and it was preferably localized in the cell periphery.

We have shown that SLNs are nontoxic in CDR1 mice, when orally or intravenously administered. Biodistribution assays showed a homogeneous fluorescence distribution from intravenous IR780-loaded SLNs in the whole animal, without organ specific fluorescence accumulation. Oral administration only provided fluorescence signal in the gastrointestinal area. It suggests that SLNs were not absorbed at intestinal level to the blood stream, or that concentration was not enough to provide a detectable signal. These results indicate the great potential of MA-based SLNs as nanocarriers of anticancer drugs. Moreover, they constitute a useful and promising platform to implement targeted theranostic systems based on functionalizing with homing peptides or antibodies against specific tumor cells.

Funding Source

All sources of funding should be acknowledged, and you should declare any extra funding you have received for academic research of this work. If there are none state ‘there are none’.

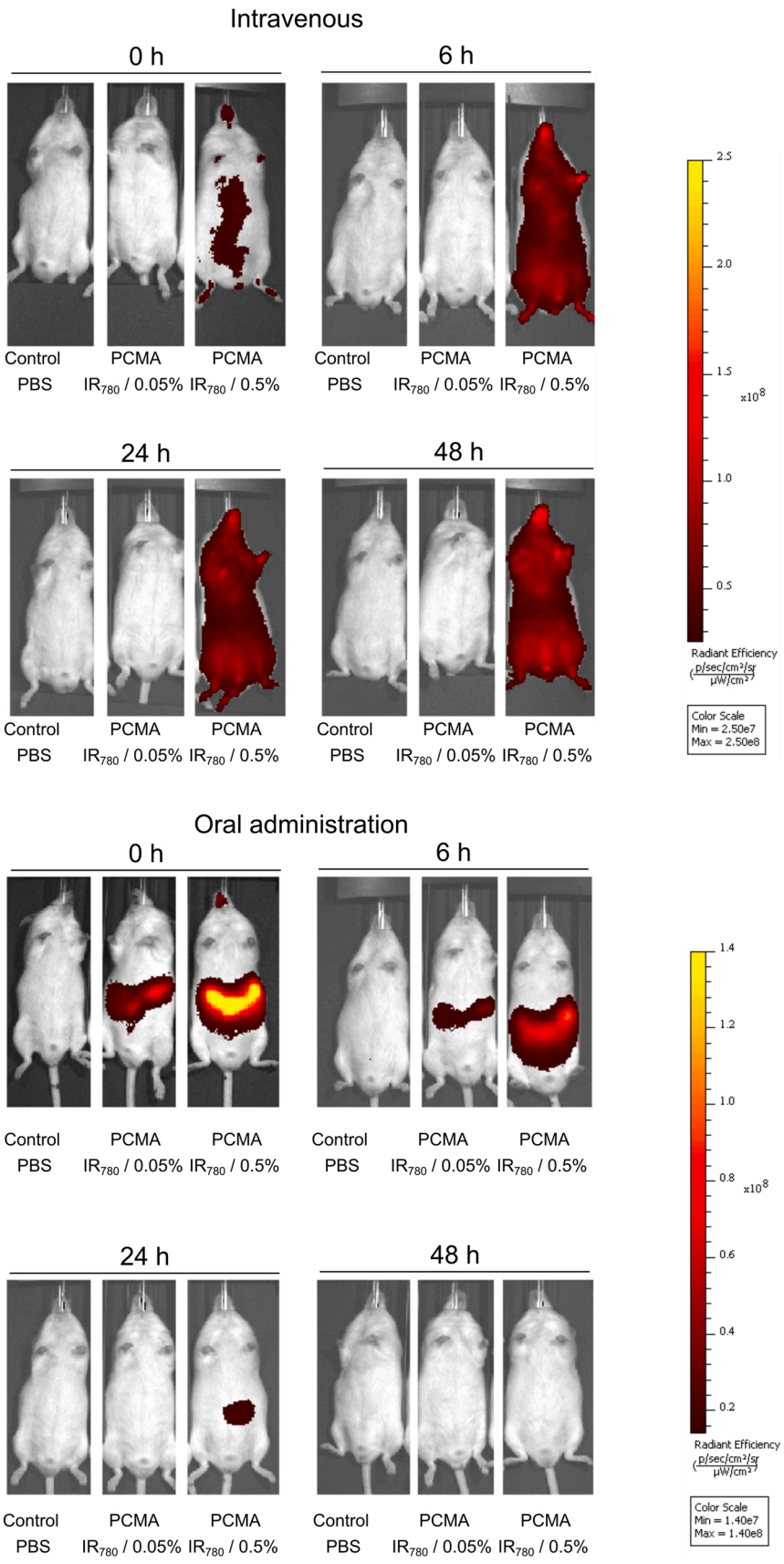

Figure 7. IVIS® (Perkin Elmer) images of the biodistribution of IR780-PCMA in healthy male CD1 mice after oral or intravenous administration with one dose of IR780-PCMA (0.4 mg of MA with 0.05 or 0.5% w/w IR780). Control mouse was intravenously administered with PBS.

CRediT authorship contribution statement

Aixa Aguilera-Garrido: Investigation, Conceptualization, Validation, Data curation, Formal analysis, Visualization, Writing – original draft. **Pablo Graván:** Investigation, Conceptualization, Validation, Data curation, Formal analysis, Visualization, Writing – original draft. **Saúl A. Navarro-Marchal:** Supervision, Investigation, Conceptualization, Writing – review & editing. **Marta Medina-O'Donnell:** Supervision, Resources, Writing – review & editing. **Andrés Parra:** Supervision, Resources, Writing – review & editing. **María José Gálvez-Ruiz:** Resources, Conceptualization, Funding acquisition, Project administration, Supervision, Writing – review & editing. **Juan Antonio Marchal:** Resources, Conceptualization, Funding acquisition, Project administration, Supervision, Writing – review & editing. **Francisco Galisteo-González:** Resources, Conceptualization, Funding acquisition, Project administration, Supervision, Writing – review & editing.

Declaration of Competing Interest

Please declare any financial or personal interests that might be potentially viewed to influence the work presented. Interests could include consultancies, honoraria, patent ownership or other. If there are none state 'there are none'.

Acknowledgement

This work was supported by the projects RTI2018. 101309B - C21 and RTI2018. 101309B - C22 funded by MCIN / AEI / 10.13039 / 501100011033/ FEDER "Una manera de hacer Europa" and by the Chair "Doctors Galera-Requena in cancer stem cell research". P. Graván acknowledges the Ph.D. student fellowship (FPU18/05336) from MCIN/AEI/10.13039/501100011033 and FSE.

Appendix A. Supporting information

Supplementary data associated with this article can be found in the online version at doi:10.1016/j.biopha.2023.114828.

References

[1] D.J. Newman, G.M. Cragg, J. Nat. Prod. 70 (2007) 461–477, https://doi.org/10.1021/np068054v.
[2] M. Sánchez-González, G. Lozano-Mena, M.E. Juan, A. García-Granados, J. M. Planas, Mol. Nutr. Food Res. 57 (2013) 339–346, https://doi.org/10.1002/mnfr.201200481.
[3] A. García-Granados, A. Martínez, J.N. Moliz, A. Parra, F. Rivas, Molecules (1998) 3.
[4] G. Lozano-Mena, M. Sánchez-González, M.E. Juan, J.M. Planas, Molecules 19 (2014) 11538–11559, https://doi.org/10.3390/molecules190811538.
[5] X.Z. Tang, T. Guan, Y.S. Qian, Y.M. Li, H.B. Sun, J.H. Huang, Y. Zhang, Chin. J. Nat. Med. 6 (2008) 53–56, https://doi.org/10.1016/S1875-5364(09)60005-4.
[6] C. García-Granados, A.; Martínez, A.; Parra, A.; Rivas, F.; Osuna, A.; Mascaró, 1999.
[7] A. MárquezMartín, R. de la Puerta Vázquez, A. Fernández-Arche, V. Ruiz-Gutiérrez, Free Radic. Res. 40 (2006) 295–302, https://doi.org/10.1080/10715760500467935.
[8] C. Sánchez-Quesada, A. López-Biedma, F. Warleta, M. Campos, G. Beltrán, J. J. Gaforio, J. Agric. Food Chem. 61 (2013) 12173–12182, https://doi.org/10.1021/jf403154e.
[9] M. Medina-O'Donnell, F. Rivas, F.J. Reyes-Zurita, A. Martinez, F. Galisteo-González, J.A. Lupiañez, A. Parra, Fitoterapia 120 (2017) 25–40. ⟨http://hdl.handle.net/10481/48438⟩.
[10] M.E. Juan, U. Wenzel, V. Ruiz-Gutierrez, H. Daniel, J.M. Planas, J. Nutr. 136 (2018) 2553–2557, https://doi.org/10.1093/jn/136.10.2553.
[11] X. He, H.L. Rui, J. Agric. Food Chem. 55 (2007) 4366–4370, https://doi.org/10.1021/jf063563o.
[12] R. Martín, J. Carvalho, E. Ibeas, M. Hernández, V. Ruiz-Gutierrez, M.L. Nieto, Cancer Res. 67 (2007) 3741–3751, https://doi.org/10.1158/0008-5472.CAN-06-4759.
[13] J.A. Salvador, A.S. Leal, D.P. Alho, B.M. Gonçalves, A.S. Valdeira, V.I. Mendes, Y. Jing, Studies in Natural ProductsChemistry, Elsevier,, 2014, pp. 33–73, https://doi.org/10.1016/B978-0-444-63294-4.00002-4, vol. 41.
[14] B.S. Gill, S. Kumar, Navgeet, Mol. Biol. Rep. 43 (2016) 881–896, https://doi.org/10.1007/s11033-016-4032-9.
[15] K.C. Lai, S.F. Peng, C.C. Liu, J.Y. Huang, J.Y. Kuo, Z.Y. Cheng, R.S.C. Wu, C.C. Lin, J.K. Chen, J.G. Chung, InVivo 33 (2019) 65–73, https://doi.org/10.21873/invivo.11440.
[16] C. Li, Z. Yang, C. Zhai, W. Qiu, D. Li, Z. Yi, L. Wang, J. Tang, M. Qian, J. Luo, M. Liu, Mol. Cancer 9 (2010) 1–13, https://doi.org/10.1186/1476-4598-9-73.
[17] S. Sánchez-Tena, F.J. Reyes-zurita, S. Díaz-Moralli, M.P. Vinardell, M. Reed, F. García-García, J. Dopazo, J.A. Lupiáñez, U. Günther, M. Cascante, PLoS ONE 8 (2013), e59392, https://doi.org/10.1371/journal.pone.0059392.
[18] K.X. Ooi, C.L. Poo, M. Subramaniam, G.A. Cordell, Y.M. Lim, Phytomedicine 110 (2023), 154631, https://doi.org/10.1016/j.phymed.2022.154631.
[19] W. Mehnert, K. Mader, Adv. Drug Deliv. Rev. 47 (2001) 165–196, https://doi.org/10.1016/S0169-409X(01)00105-3.
[20] P. Graván, A. Aguilera-Garrido, J.A. Marchal, S.A. Navarro-Marchal, F. Galisteo-González, Adv. Colloid Interface Sci. 314 (2023), 102871, https://doi.org/10.1016/j.cis.2023.102871.
[21] S. Nasirizadeha, B. Malaekeh-Nikouei, J. Drug Deliv. Technol. 55 (2020), 101458, https://doi.org/10.1016/j.jddst.2019.101458.
[22] L. Battaglia, M. Gallarate, Expert Opin. Drug Deliv. 9 (2012) 497–508, https://doi.org/10.1517/17425247.2012.673278.
[23] H. Fessi, F. Puisieux, J. Devissaguet, N. Ammoury, S. Benita, Int. J. Pharm. 55 (1989) R1–R4, https://doi.org/10.1016/0378-5173(89)90281-0.
[24] F. Curt, D. Jean-Philipe, P. Francis and T. Curt, 1992, US-5118528-A.
[25] E. Giuliano, D. Paolino, M. Fresta, D. Cosco, Pharmaceutics 10 (2018) 1–26, https://doi.org/10.3390/pharmaceutics10030159.
[26] M. Wulff-Pérez, J. de Vicente, A. Martín-Rodríguez, M.J. Gálvez-Ruiz, Int. J. Pharm. 423 (2012) 161–166, https://doi.org/10.1016/j.ijpharm.2011.12.025.
[27] A. Torcello-Gómez, M. Wulff-Pérez, M.J. Gálvez-Ruiz, A. Martín-Rodríguez, M. Cabrerizo-Vílchez, J. Maldonado-Valderrama, Adv. Colloid Interface Sci. 206 (2014) 414–427, https://doi.org/10.1016/j.foodhyd.2012.12.026.
[28] D.E. Owens, N.A. Peppas, Int. J. Pharm. 307 (2006) 93–102, https://doi.org/10.1016/j.ijpharm.2005.10.010.
[29] M.J. Santander-Ortega, M.V. Lozano-López, D. Bastos-González, J.M. Peula-García, J.L. Ortega-Vinuesa, Colloid Polym. Sci. 288 (2010) 159–172, https://doi.org/10.1007/s00396-009-2132-y.
[30] M.N. Khalid, P. Simard, D. Hoarau, A. Dragomir, J.-C. Leroux, Pharm. Res. 23 (2006) 752–758, https://doi.org/10.1007/s11095-006-9662-5.
[31] W. Punfa, S. Yodkeeree, P. Pitchakarn, C. Ampasavate, P. Limtrakul, Acta Pharmacol. Sin. 33 (2012) 823–831, https://doi.org/10.1038/aps.2012.34.
[32] M.A. Tomeh, R. Hadianamrei, X. Zhao, Int. J. Mol. Sci. 20 (2019) 1033, https://doi.org/10.3390/ijms20051033.
[33] M.G. González-Pedroza, L. Argueta-Figueroa, R. García-Contreras, Y. Jiménez-Martínez, E. Martínez-Martínez, S.A. Navarro-Marchal, J.A. Marchal, R.A. Morales-Luckie, H. Boulaiz, Nanomaterials 11 (2021) 1–17, https://doi.org/10.3390/nano11051273.
[34] C.W. Extrand, Langmuir 21 (2005) 10370–10374, https://doi.org/10.1021/la0513050.
[35] E. Lepeltier, C. Bourgaux, P. Couvreur, Adv. Drug Deliv. 71 (2014) 86–97, https://doi.org/10.1016/j.addr.2013.12.009.
[36] S. Salatin, A. Yari Khosroushahi, J. Cell. Mol. Med. 21 (2017) 1668–1686, https://doi.org/10.1111/jcmm.13110.
[37] P. Legrand, S. Lesieur, A. Bochot, R. Gref, W. Raatjes, G. Barrattand, C. Vauthier, Int. J. Pharm. 344 (2007) 33–43, https://doi.org/10.1016/j.ijpharm.2007.05.054.
[38] O. Thioune, H. Fessi, J. Devissaguet, F. Puisieux, Int. Pharm. 146 (1997) 233–238, https://doi.org/10.1016/S0378-5173(96)04830-2.
[39] H. Lannibois, A. Hasmy, R. Botet, O.A. Chariol, B. Cabane, J. De. Phys. I 7 (1997) 319–342, https://doi.org/10.1051/jp2:1997128.
[40] X. Huang, C.S. Brazel, J. Control. Release 73 (2001) 121–136, https://doi.org/10.1016/S0168-3659(01)00248-6.
[41] R.H. Müller, M. Radtke, S.A. Wissing, Int. J. Pharm. 242 (2002) 121–128, https://doi.org/10.1016/S0378-5173(02)00180-1.
[42] M. DeiCas, R. Ghidoni, Nutrients 11 (2019) 2147, https://doi.org/10.3390/nu11092147.
[43] S.J. Stohs, O. Chen, S.D. Ray, J. Ji, L.R. Bucci, H.G. Preuss, Molecules 25 (2020) 1397, https://doi.org/10.3390/molecules25061397.
[44] M. Medina-O'Donnell, PhD thesis, University of Granda, ⟨http://hdl.handle.net/10481/48438⟩, 2017.⟨http://hdl.handle.net/10481/48438⟩.
[45] M.F. Attia, N. Anton, J. Wallyn, Z. Omran, T.F. Vandamme, J. Pharm. Pharmacol. 71 (2019) 1185–1198, https://doi.org/10.1111/jphp.13098.
[46] P.L.C. Michelle Longmireand, H. Kobayashi, Nanomedicine 3 (2012) 703–717, https://doi.org/10.2217/17435889.3.5.703.Clearance.
[47] S. Quesada, C. López-Biedma A, J.J. Gaforio, Evid. -Based Complement. Altern. Med. 2015 (2015), 654721, https://doi.org/10.1155/2015/654721.
[48] J. Yoon, A. Kanamori, K. Fujii, H. Isoda, T. Okura, 2018 Mar 20, PLoS One 13 (3) (2018), e0194572, https://doi.org/10.1371/journal.pone.0194572.
[49] N. Nagai, S. Yagyu S, A. Hata, S. Nirengi, K. Kotani, T. Moritani, N. Sakane, J. Clin. Biochem Nutr. 64 (3) (2019) 224–230, https://doi.org/10.3164/jcbn.18-104.
[50] S. Fukumitsu, T. Kinoshita, M.O. Villarea, K. Aida, A. Hino, H. Isoda, J. Clin. Biochem Nutr. 61 (1) (2017) 67–73, https://doi.org/10.3164/jcbn.16-119. Epub 2017 May 16. PMID: 28751812; PMCID: PMC5525013.
[51] Y. Yamauchi, F. Ferdousi, S. Fukumitsu, H. Isoda, Nutrients 13 (9) (2021) 2950, https://doi.org/10.3390/nu13092950.
[52] M.E. Juan, G. Lozano-Mena, M. Sanchez-Gonzalez, J.M. Planas, Molecules 24 (7) (2019) 1266, https://doi.org/10.3390/molecules24071266.
[53] X. Bai, Y. Zhang, H. Jiang, P. Yang, H. Li, Y. Zhang, P. He, Mol. Med. Rep. 13 (2016) 117–122, https://doi.org/10.3892/mmr.2015.4552.

[54] F.J. Reyes-Zurita, E.E. Rufino-Palomares, J.A. Lupiañez, M. Cascante, Cancer Lett. 273 (2009) 44–54, https://doi.org/10.1016/j.canlet.2008.07.033.
[55] M.E. Juan, Planas V. Ruiz-Gutierrez, H. Daniel, U. Wenzel, Br. J. Nutr. 100 (2008) 36–43, https://doi.org/10.1017/S0007114508882979.
[56] F.J. Reyes-Zurita, E.E. Rufino-Palomares, L. Garcia-Salguero, J. Peragon, P. P. Medina, A. Parra, M. Cascante, J.A. Lupiañez, PLOS ONE 11 (2016) 1–16, https://doi.org/10.1371/journal.pone.0146178.
[57] Q. Wei, B. Zhang, P. Li, X. Wen, J. Yang, J. Agric. Food Chem. 67 (2019) 4259–4272, https://doi.org/10.1021/acs.jafc.9b00170.
[58] X. Zhang, G. Chen, T. Zhang, Z. Ma, B. Wu, Int J. Nanomed. 9 (2014) 5503–5514, https://doi.org/10.2147/IJN.S73340.
[59] P. Thakor, W. Song, R.B. Subramanian, V.R. Thakkar, D.A. Vesey, G.C. Gobe, J. Kidney Cancer VHL 4 (2017) 16–24, https://doi.org/10.15586/jkcvhl.2017.64.
[60] M. Zhang, S. Gao, D. Yang, Y. Fang, X. Lin, X. Jin, Y. Liu, X. Liu, K. Su, K. Shi (Hot Topic Reviews in Drug Delivery), Acta Pharm. Sin. B 11 (2021) 2265–2285, https://doi.org/10.1016/j.apsb.2021.03.033.
[61] Y. Yu, J. Wang, N. Xia, B. Li, X. Jiang, Oncol. Rep. 33 (2015) 1683–1690, https://doi.org/10.3892/or.2015.3755.
[62] J. Li, M.G. Wientjes, L.S. Jessie, AAPS J. 12 (2010) 223–232, https://doi.org/10.1208/s12248-010-9181-5.
[63] K. Wang, X. Zhu, Y. Yin, Front. Pharmacol. 11 (2020), https://doi.org/10.3389/fphar.2020.00835.
[64] A. Albanese, W.C. Chan, ACS Nano 5 (2011) 5478–5489, https://doi.org/10.1021/nn2007496.
[65] V. Forest, J. Pourchez, Mater. Sci. Eng. C. 70 (2017) 889–896, https://doi.org/10.1016/j.msec.2016.09.016.
[66] P. Sánchez-Moreno, PhD thesis, Granada, 2014.
[67] V. Muralidharan-Chari, H.G. Kohan, A.G. Asimakopoulos, T. Sudha, S. Sell, K. Kannan, M. Boroujerdi, P.J. Davis, S.A. Mousa, Oncotarget 7 (2016) 50365–50379, https://doi.org/10.18632/oncotarget.10395.
[68] S. Behzadia, V. Serpooshan, W. Tao, M.A. Hamaly, M.Y. Alkawareek, E.C. Dreaden, D. Brown, A.M. Alkilany, O.C. Farokhzad, M. Mahmoudi, Chem. Soc. Rev. 46 (2017) 4218–4244, https://doi.org/10.1039/c6cs00636a.
[69] A.S. Al Khafaji, M.D. Donovan, Pharmaceutics 13 (2021) 761, https://doi.org/10.3390/pharmaceutics13050761.
[70] G.H. Chai, Y. Xu, S.Q. Chen, B. Cheng, F.Q. Hu, J. You, Y.Z. Du, H. Yuan, ACS Appl. Mater. Interfaces 8 (9) (2016) 5929–5940, https://doi.org/10.1021/acsami.6b00821.
[71] A. Ramírez, H. Boulaiz, C. Morata-Tarifa, M. Perán, G. Jiménez, M. Picon-Ruiz, A. Agil, O. Cruz-López, A. Conejo-García, J.M. Campos, A. Sánchez, M.A. García, J. A. Marchal, Oncotarget 5 (11) (2014) 3590–3606, https://doi.org/10.18632/oncotarget.1962.
[72] M. Sánchez-González, G. Lozano-Mena, A. Parra, M.E. Juanand, J.M. Planas, J. Agric. Food Chem. 63 (2015) 1126–1132, https://doi.org/10.1021/jf505379g.
[73] S. Guo, L. Huang, J. Nanomater. (2011), 742895, https://doi.org/10.1155/2011/742895.
[74] A. Aguilera-Garrido, E. Arranz, M.J. Gálvez-Ruiz, J.A. Marchal, F. Galisteo-González, L. Giblin, Drug Deliv. 29 (1) (2022) 1971–1982, https://doi.org/10.1080/10717544.2022.2086937.